

## Corner Bent Integrated Design of 4G LTE and mmWave 5G Antennas for Mobile Terminals

Muhammad I. Magray<sup>1, \*</sup>, Gulur S. Karthikeya<sup>2</sup>, Khalid Muzaffar<sup>1</sup>, and Shiban K. Koul<sup>2</sup>

**Abstract**—Co-design of corner bent Multiple-Input Multiple-Output (MIMO) antennas catering to 4G LTE and mmWave 5G applications is proposed. The 4G LTE MIMO antenna module consists of two element microstrip-fed slot antennas operating from 1.7 to 3 GHz with fractional bandwidth of 55%, which covers LTE1900, LTE2300, and LTE2500 bands. For mmWave 5G MIMO antenna module, two element Vivaldi antennas with wideband operating from 25 to 38 GHz and fractional bandwidth of 41% are proposed. The mmWave 5G microstrip fed Vivaldi MIMO antennas exhibit orthogonal pattern diversity at 28 GHz with 1-dB gain bandwidth of 28%. The single element corner bent co-designed antenna is compact having dimensions of  $14 \times 51 \times 0.254 \text{ mm}^3$ . The 4G LTE and mmWave 5G antennas are electrically close to each other by  $0.01\lambda$  at 1.7 GHz for minimal physical footprint. Co-designed 4G LTE and mmWave MIMO antennas are integrated inside a typical mobile case. Simulated and measured results are presented.

### 1. INTRODUCTION

The wide explosion in the usage of smartphones has led researchers across the planet to design and develop future transceivers with high data rates. New technologies for smartphones are evolving which has provoked microwave engineers to design antenna architectures which should possess Long Term Evolution (LTE) for both voice and data applications. LTE technology comprises various operational frequency bands like LTE700 (698–787 MHz), LTE1700 (1710–2170 MHz), LTE2300 (2300–2400 MHz), and LTE2500 (2500–2690 MHz) [1]. Design of 4G LTE antennas typically has large physical footprint that limits their integration in smartphones. The mmWave 5G technology is one of the optimal choices to achieve higher data rates as it uses higher carrier frequencies. 28 GHz frequency band is of high interest for deployment of mmWave 5G antennas [2]. In addition to this, Multiple-Input Multiple-Output (MIMO) technique is a conventional method to enhance data rate. Thus, due to availability of higher data rates, future transceivers should be compatible with both 4G LTE and mmWave 5G antennas. Co-existence of 4G LTE and mmWave 5G MIMO antennas on the same module is an important problem to address backward compatibility of future smartphones [3]. Due to availability of limited space in mobile phones, integrating 4G LTE and mmWave 5G antenna architectures on the same module is challenging. Designs reported in [2, 4] have implemented the co-design architecture of 4G LTE and mmWave 5G antennas, but they have large physical footprint which is not attributed to orthogonal pattern diversity for using smartphone in portrait as well as landscape mode. In addition to this, gain at mmWave frequencies in the reported work is low. Hence, an integrated design of corner bent compact 4G LTE and high gain mmWave 5G MIMO antenna module is proposed in this paper.

---

*Received 26 June 2019, Accepted 13 August 2019, Scheduled 29 August 2019*

\* Corresponding author: Muhammad Idrees Magray (idreesmagrey@gmail.com).

<sup>1</sup> Department of Electronics and Communication Engineering, Islamic University of Science & Technology, Awantipora, J&K, India.

<sup>2</sup> Centre for Applied Research in Electronics (CARE), Indian Institute of Technology (IIT) Delhi, Hauz Khas, New Delhi, India.

## 2. 4G LTE AND MMWAVE 5G CORNER BENT MIMO ANTENNA DESIGN

Antenna designs and simulations are carried out in Computer Simulation Technology (CST) Microwave Studio (MS). Proposed 4G LTE and mmWave 5G MIMO antenna architecture is designed on a 10-mil thick Rogers 5870 substrate with dielectric constant ( $\epsilon_r$ ) of  $2.33 \pm 0.02$  and loss tangent of 0.0012. Substrate of low relative permittivity is chosen in order to minimize surface wave modes. In addition to this, low radiation efficiency is also the consequence of using the substrate of high dielectric constant and high loss tangent [5]. Further, a 10-mil substrate is used as it is the optimal choice for achieving corner bending. Electrically thin substrate is chosen in order to decrease cross polarization [6]. On the other hand, 5-mil substrate being more flexible than the proposed substrate requires additional scaffolding [7]. Flexible substrates like polyethylene terephthalate (PET) and polycarbonate have high loss tangent, which will result in additional gain deterioration at mmWave frequencies [8].

### 2.1. 4G LTE Antenna Design

Schematics of the proposed 4G LTE antenna integrated with mmWave 5G antenna module is depicted in Figs. 1(a) and (b) with top and bottom planes, respectively. Proposed 4G LTE section of the antenna is electrically small having dimensions of  $0.08\lambda \times 0.17\lambda \times 0.001\lambda$  at 1.7 GHz. A rectangular slot of proper dimensions is etched on the ground plane which is excited by  $5\ \Omega$  microstrip line on the other plane. The proposed 4G LTE slot antenna achieves resonance depending upon the relative position of microstrip feed, width of rectangular slot ( $D$ ), and length of feed line ( $L$ ). Optimized dimensions for feed length ( $L$ ) and rectangular slot width ( $D$ ) as depicted in Figs. 1(a) and (b) are obtained to be 12.5 mm and 1 mm, respectively. Plots of input reflection coefficient ( $|S_{11}|$ ) on variation of length of feed line ( $L$ ) and width of slot ( $D$ ) are shown in Figs. 2(a) and (b), respectively.

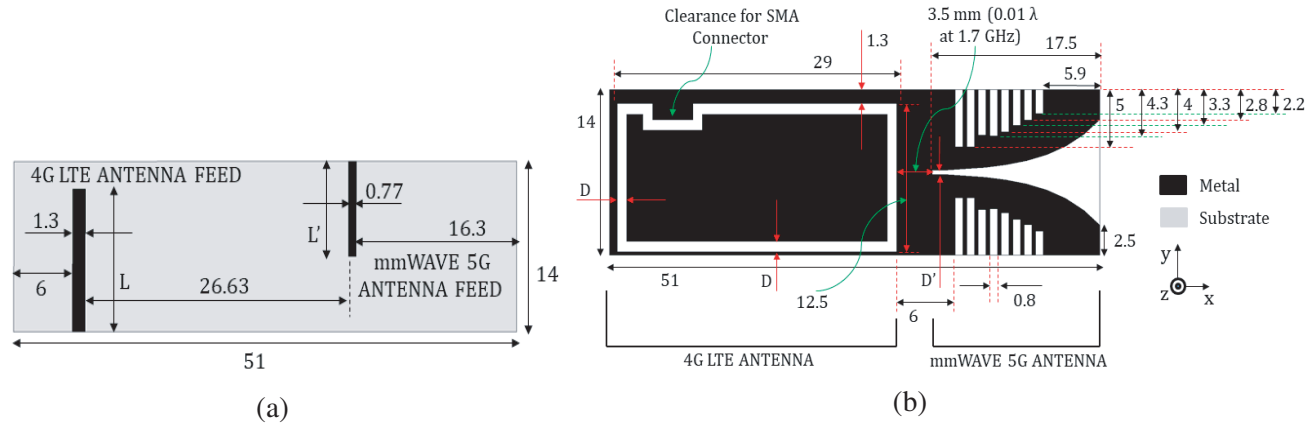


**Figure 1.** Schematics of the proposed integrated 4G LTE and mmWave 5G antenna, (a) top plane and (b) bottom plane (All dimensions are in mm).

The proposed co-designed 4G LTE and mmWave 5G antenna is fabricated, and photographs are shown in Figs. 3(a) and (b) with top and bottom planes, respectively. Simulated and measured input reflection coefficients of the proposed 4G LTE antenna are illustrated in Fig. 4(a). Measured results are carried out using Agilent PNA E8364C. Measured impedance bandwidth of the proposed 4G LTE antenna is from 1.7 to 3 GHz. The proposed antenna is wideband having fractional bandwidth of 55%. The proposed prototype covers multiple LTE bands like LTE1700 (1710–2170 MHz), LTE2300 (2300–2400 MHz), and LTE2500 (2500–2690 MHz) thus making carrier aggregation possible for achieving higher data rates. Discrepancies between simulated and measured data may be due to fabrication tolerances. Also, frequency shift may be due to inhomogeneity of relative permittivity of the substrate [9].

Broadside gain and radiation efficiency plots of the proposed antenna are depicted in Fig. 4(b). Gain of the proposed antenna at the operating LTE bands lies between 1.7 and 2.1 dBi indicating high gain

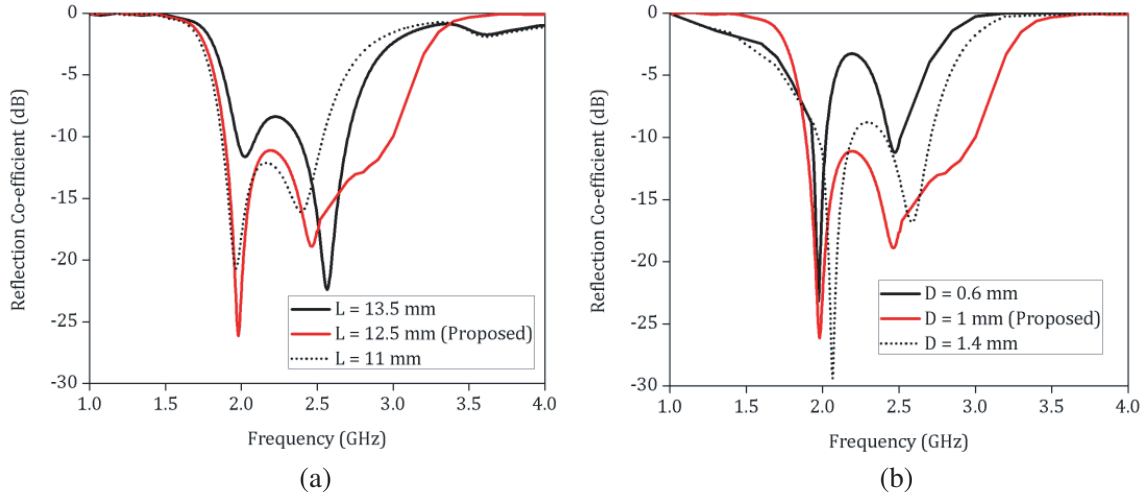


**Figure 2.** Input reflection co-efficient plot of the proposed 4G LTE antenna on variation of (a) length of feed line ( $L$ ) and (b) width of rectangular slot ( $D$ ).

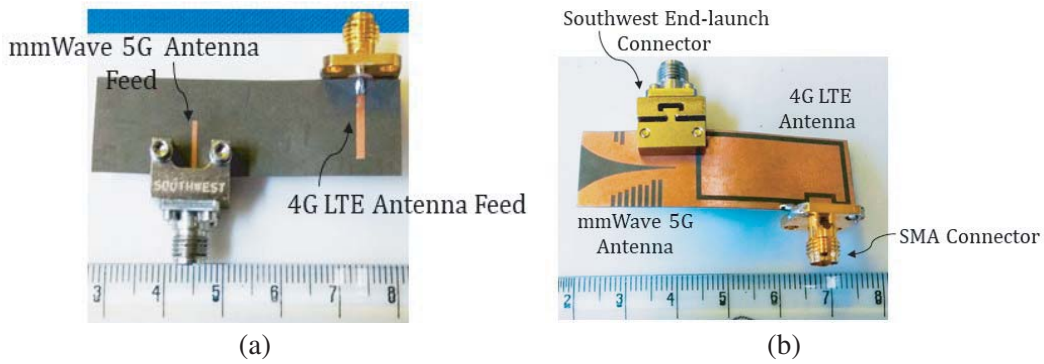


**Figure 3.** Photograph of the fabricated co-designed 4G LTE and mmWave 5G antenna, (a) top plane and (b) ground plane.

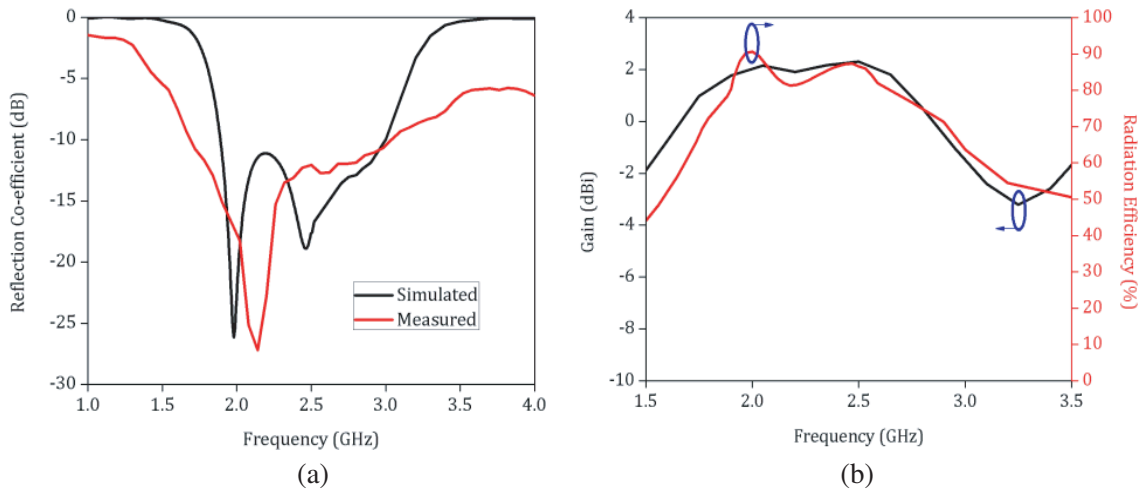


**Figure 4.** (a) Input reflection co-efficient and (b) gain and radiation efficiency plots of the proposed 4G LTE antenna.

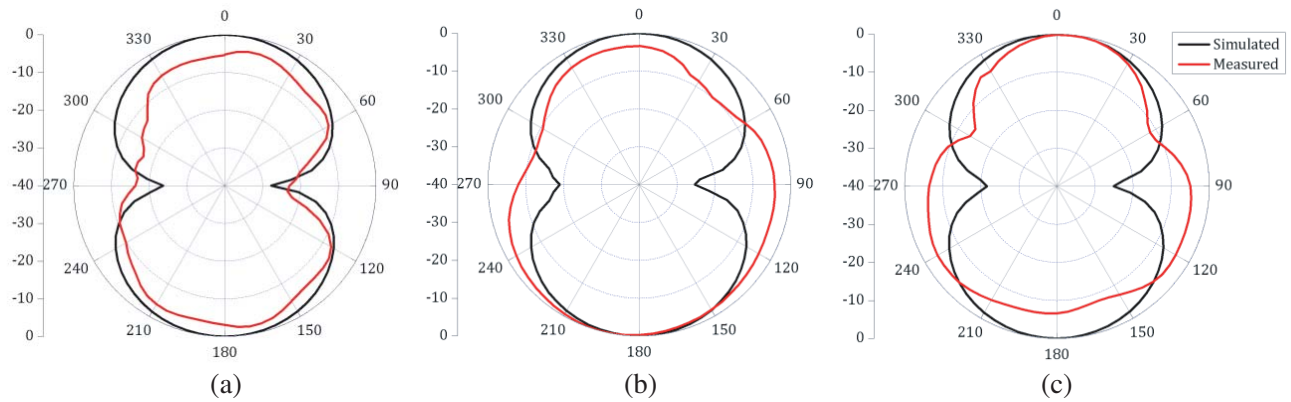


**Figure 5.** Simulated and measured radiation plots in  $YZ$ -plane at (a) 1.8 GHz, (b) 2.3 GHz and (c) 2.6 GHz.

yield for the given electrical size. In addition to this, radiation efficiency at the catered LTE bands lies between 60 and 85%. High efficiency of the proposed antenna is due to the electrically thin substrate with low dissipation factor. Simulated and measured radiation patterns of the proposed antenna in  $YZ$ -plane ( $E$ -plane) are illustrated in Fig. 5. Measured results are obtained in an anechoic chamber. The proposed antenna achieves pattern integrity with dipole-like radiation patterns. Disparity between simulated and measured data is due to poor absorptivity of oblique incidence in the anechoic chamber.

## 2.2. mmWave 5G Antenna Design

Tapered slot antenna with end-fire gain is designed for mmWave 5G applications. Schematics of the proposed mmWave 5G antenna co-designed with 4G LTE antenna are shown in Figs. 1(a) and (b) with top and ground planes, respectively. The proposed mmWave 5G section of the antenna has dimensions of  $1.75\lambda \times 1.4\lambda \times 0.0254\lambda$  at 28 GHz. Tapered slot antenna is a traveling wave antenna [10].  $50\ \Omega$  microstrip line feeds the balun of Vivaldi antenna, and microstrip to slot line transition is optimized for better impedance matching. Optimized dimensions for length of feed line ( $L'$ ) and width of slot line ( $D'$ ) as illustrated in Figs. 1(a) and (b) are obtained to be 8.5 mm and 0.4 mm, respectively. Effects of parameters, feed length ( $L'$ ), and slot line width ( $D'$ ), on input reflection coefficient are shown in Figs. 6(a) and (b).

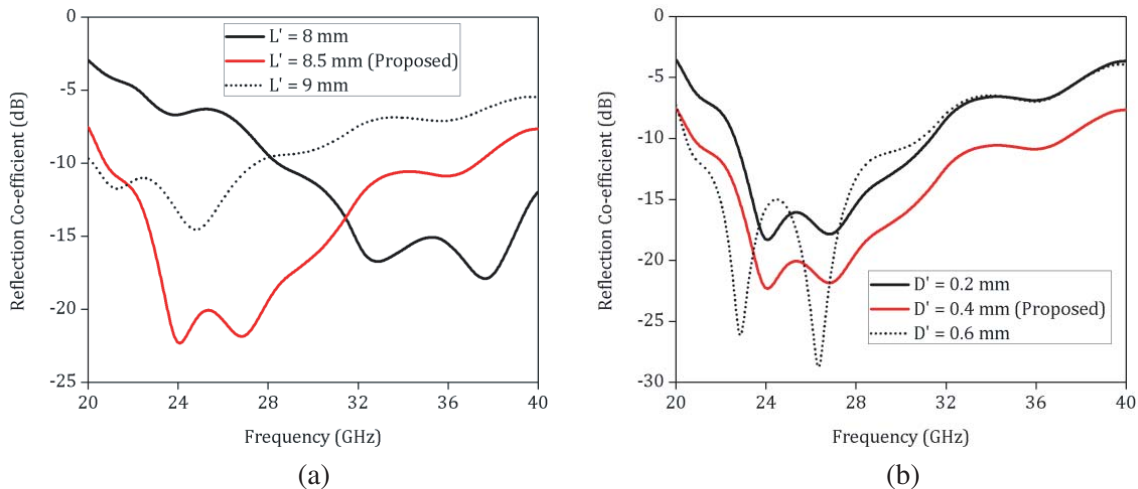


**Figure 6.** Input reflection coefficient plot of the proposed mmWave 5G antenna on variation of (a) length of feed line ( $L'$ ) and (b) slot line width ( $D'$ ).

The proposed antenna consists of exponentially tapered in the ground plane. Proposed antenna starts radiating from the metallic taper until electromagnetic wave travels around half of the wavelength [11]. Corrugations are inserted in the proposed antenna in order to concentrate the E-field towards the main radiating aperture thereby reducing back lobe. Thus, cross polarization and side-lobe levels for the proposed antenna are reduced [12]. E-field plot at 28 GHz is depicted in Fig. 7 that justifies the traveling nature of antenna.

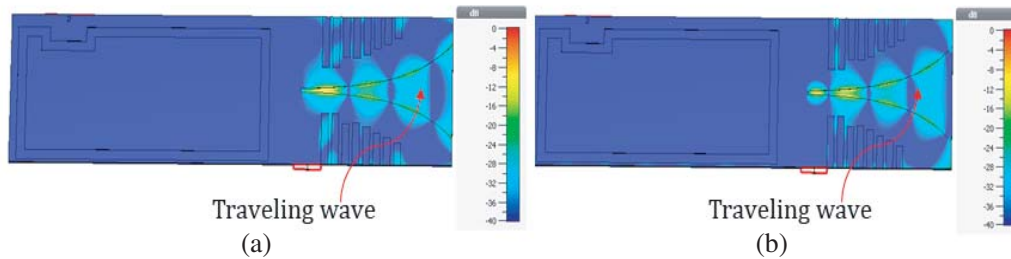


**Figure 7.** E-field plots for the proposed mmWave 5G antenna at (a)  $t = 0$  and (b)  $t = T/4$ .

Photographs of the proposed mmWave 5G antenna are shown in Figs. 3(a) and 3(b) with top and bottom planes respectively. Simulated and measured input reflection coefficients of the proposed antenna are illustrated in Fig. 8(a). Measured impedance bandwidth is high ranging from 25 to 38 GHz with fractional bandwidth of 41%. Discrepancies can be imputed to fabrication tolerances and deviation in port impedance offered by end-launch connector [13]. Gain of the proposed antenna lies between 9 and 10.5 dBi indicating high gain for the available aperture as depicted in Fig. 8(b). Moreover, 1-dB gain bandwidth of the proposed antenna is around 28% with gain varying between 9.5 and 10.5 dBi. Standard gain transfer method is used for gain measurement using Keysight horn antennas. As path loss is high at mmWave frequencies, mobile phone antennas must possess high gain. Also, efficiency for the proposed antenna is high ranging between 80 and 88% as shown in Fig. 8(b).

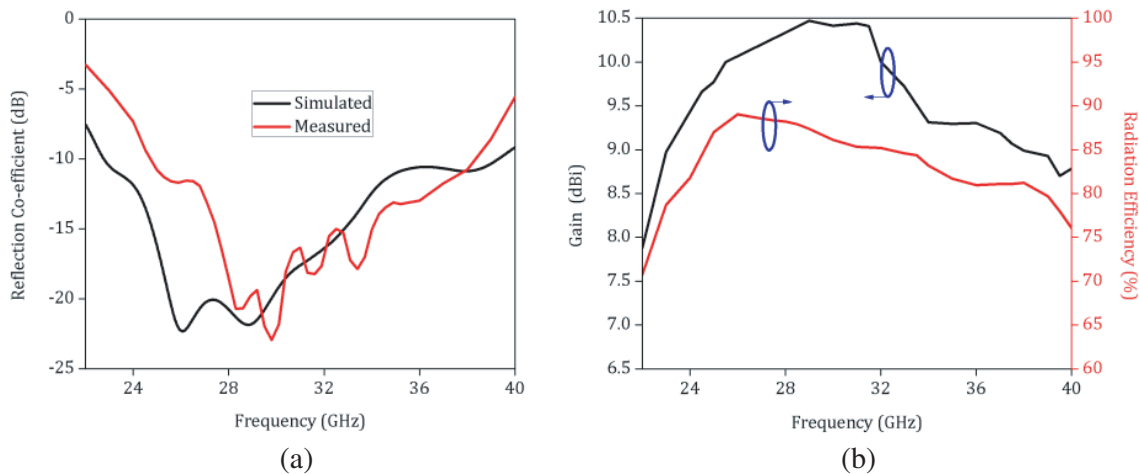


**Figure 8.** (a) Input reflection co-efficient and (b) gain and radiation efficiency plots of the proposed mmWave 5G antenna.

Traveling wave phenomenon is realized as illustrated in Fig. 7 with traveling wave propagating at two different time instants. Simulated and measured radiation patterns of the proposed mmWave 5G antenna in  $XY$ -plane at 28, 33 and 38 GHz are depicted in Fig. 9. The proposed antenna shows pattern integrity at all the three given frequencies. Front to back ratio of the proposed tapered slot antenna is greater than 15 dB. Disparity between simulated and measured patterns is due to alignment errors and adapters used for pattern measurement.

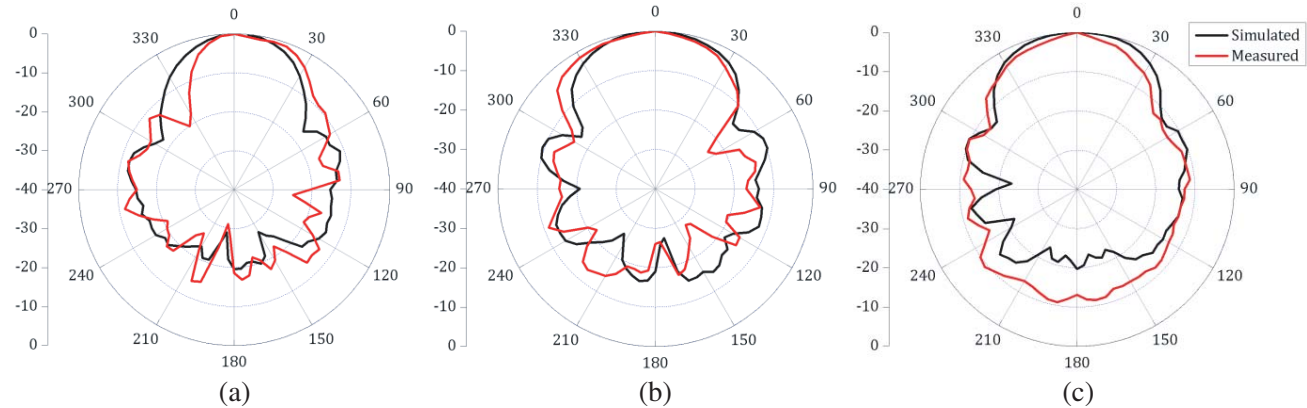


**Figure 9.** Simulated and measured radiation plots in  $XY$ -plane at (a) 28 GHz, (b) 33 GHz and (c) 38 GHz.

### 2.3. Co-Designed Corner Bent 4G LTE and mmWave 5G MIMO Antenna Design

Proposed 4G LTE and mmWave 5G antennas are integrated with each other on the same 10-mil Rogers 5870 substrate and separated by a distance of 3.5 mm. Separation between co-designed antennas can be further reduced, but due to the bulky size of end-launch connector, clearance is maintained in order to mount the connector for measurements at mmWave frequencies [14]. Corner bending is done in order to decrease effective radiating volume. Also, in order to fit the antenna in the corner of a typical smartphone, corner bending is achieved. Antenna characteristics are observed, and there is no significant variation in input reflection coefficient or gain of either the 4G LTE or mmWave 5G antenna. Furthermore, for analytical analysis of bending many reported articles have been investigated [15–20]. Mutual coupling between 4G LTE and mmWave 5G antennas is very minimal as can be realized from Fig. 11(a), and hence integrated antenna modules can be operated independently and/or simultaneously. Furthermore, antenna characteristics like impedance bandwidth and radiation patterns remain invariant as isolation between the co-designed antenna elements is greater than 30 dB.

For realizing corner bent MIMO configuration, another co-designed 4G LTE and mmWave element is brought to the opposite corner of smartphone as illustrated in Fig. 10. The two antenna elements are placed in such a way that orthogonal pattern diversity at mmWave frequencies is achieved as depicted in Fig. 11(b). Orthogonal pattern diversity results in the usage of mobile phone in portrait as well as

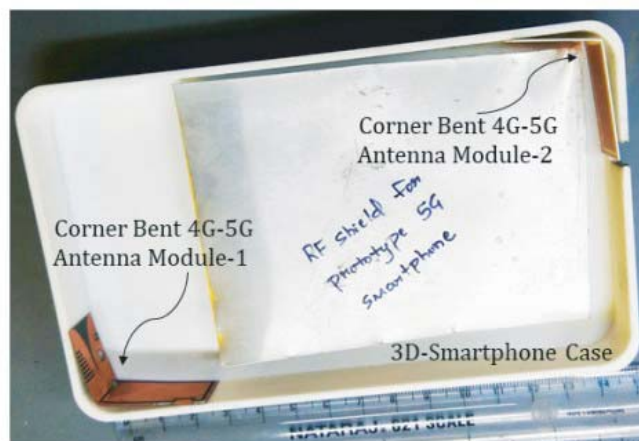


**Figure 10.** Integrated 4G LTE and mmWave 5G corner bent MIMO antenna design inside a typical mobile phone case.

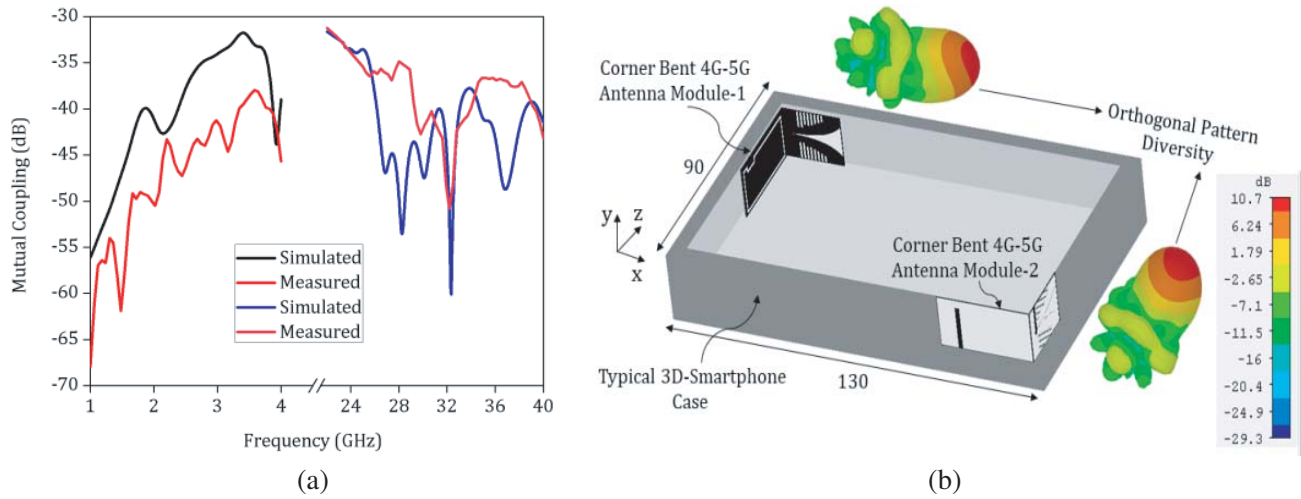


**Figure 11.** (a) Isolation plot of the co-designed 4G LTE and mmWave antenna element and (b) orthogonal pattern diversity architecture with 3D patterns at 28 GHz.

**Table 1.** Comparison of the proposed MIMO antenna design with other reported designs.

Figures of Merit	Proposed Work	[2]	[4]
<b>4G LTE ANTENNA</b>			
Volume of Single Element	$30 \times 14 \times 0.254 \text{ mm}^3$	$75 \times 8 \times 7 \text{ mm}^3$	$9 \times 30 \times 0.965 \text{ mm}^3$
Fractional Bandwidth (BW)	<b>55% (-10 dB BW)</b>	31% — Low Band, 44% — High Band (-6 dB BW)	30% (-6 dB BW)
Operating LTE Bands	<b>LTE1900/2300/2500</b>	LTE700/1900/2300/2500	LTE1900/2300/2500
Gain	<b>1.7–2.1 dBi</b>	Not Available	1.7–3.86 dBi
Efficiency	<b>60–90%</b>	50–90%	50–83%
MIMO	<b>Yes</b>	No	Yes
Corner Bent	<b>Yes</b>	No	No
<b>mmWAVE 5G ANTENNA</b>			
Volume of antenna	$17.5 \times 14 \times 0.254 \text{ mm}^3$ (Single Element)	$23 \times 7 \times 4 \text{ mm}^3$ (1 × 4 array)	$23.2 \times 8.3 \times 0.965 \text{ mm}^3$ (2 × 4 array)
Impedance Bandwidth	<b>25–38 GHz</b>	25–30 GHz	26–28.4 GHz
Peak Realized Gain	<b>10.5 dB</b>	7 dB	8.2 dB
1-dB Gain Bandwidth	<b>28%</b>	Not Available	Not Available
Efficiency	<b>80–88%</b>	Not Available	Not Available
Orthogonal Pattern Diversity	<b>Yes</b>	No	No
MIMO	<b>Yes</b>	No	No
Corner Bent	<b>Yes</b>	No	No

landscape mode. Table 1 illustrates the comparison of the proposed 4G LTE and mmWave corner bent MIMO antenna designs with other reported designs.

### 3. CONCLUSION

Corner bent integrated design of 4G LTE and mmWave MIMO antennas are proposed. The 4G LTE MIMO antenna module consists of two compact microstrip fed slot antennas, which caters to LTE1900/LTE2300 and LTE2500 frequency bands. The proposed 4G LTE antenna operates from 1.7 to 3 GHz with fractional bandwidth of 55%. Moreover, mmWave 5G MIMO antenna module consists of two wideband tapered slot antennas with impedance bandwidth from 25 to 38 GHz. 1-dB gain bandwidth of the proposed mmWave 5G antenna is around 28% with gain varying between 9.5 and 10.5 dBi indicating a high gain yield for available aperture. The proposed MIMO antenna module is integrated in a typical smartphone, which exhibits orthogonal pattern diversity. Measurement results validate that 4G LTE and mmWave 5G antenna modules operate independently without interfering with each other's performance. Thus, the proposed antenna module is a potential candidate for integrated 4G LTE and mmWave 5G applications.

### REFERENCES

1. Ji, J. K., "Compact multiband antenna employing wideband dual ZOR for mobile handset applications," *ICT Express*, Vol. 3, No. 2, 81–84, 2017.
2. Kurvinen, J., H. Kähkönen, A. Lehtovuori, J. Ala-Laurinaho, and V. Viikari, "Co-designed mm-wave and LTE handset antennas," *IEEE Transactions on Antennas and Propagation*, Vol. 67, No. 3, 1545–1553, Mar. 2019.
3. Sharawi, M. S., M. Ikram, and A. Shamim, "A two concentric slot loop based connected array MIMO antenna system for 4G/5G terminals," *IEEE Transactions on Antennas and Propagation*, Vol. 65, No. 12, 6679–6686, Dec. 2017.
4. Hussain, R., A. T. Alreshaid, S. K. Podilchak, and M. S. Sharawi, "Compact 4G MIMO antenna integrated with a 5G array for current and future mobile handsets," *IET Microw. Antennas Propag.*, Vol. 11, No. 2, 271–279, Feb. 2017.
5. Gauthier, G. P., A. Courtauy, and G. M. Rebeiz, "Microstrip antennas on synthesized low dielectric-constant substrates," *IEEE Transactions on Antennas and Propagation*, Vol. 45, No. 8, 1310–1314, Aug. 1997.
6. Alhalabi, R. A. and G. M. Rebeiz, "Differentially-fed millimeter-wave Yagi-Uda antennas with folded dipole feed," *IEEE Transactions on Antennas and Propagation* Vol. 58, No. 3, 966–969, Mar. 2010.
7. Sarabandi, K., J. Oh, L. Pierce, K. Shivakumar, and S. Lingaiah, "Lightweight, conformal antennas for robotic flapping flyers," *IEEE Antennas and Propagation Magazine*, Vol. 56, No. 6, 29–40, Dec. 2014.
8. Jilani, S. F. and A. Alomainy, "Planar millimeter-wave antenna on low-cost flexible PET substrate for 5G applications," *2016 10th European Conference on Antennas and Propagation (EuCAP)*, 1–3, Davos, 2016.
9. Zhang, C., J. Gong, Y. Li, and Y. Wang, "Zeroth-order-mode circular microstrip antenna with patch-like radiation pattern," *IEEE Antennas and Wireless Propagation Letters*, Vol. 17, No. 3, 446–449, 2018.
10. Jarufe, C., et al., "Optimized corrugated tapered slot antenna for mm-wave applications," *IEEE Transactions on Antennas and Propagation*, Vol. 66, No. 3, 1227–1235, Mar. 2018.
11. Schaubert, D., E. Kollberg, T. Korzeniowski, T. Thungren, J. Johansson, and K. Yngvesson, "Endfire tapered slot antennas on dielectric substrates," *IEEE Transactions on Antennas and Propagation*, Vol. 33, No. 12, 1392–1400, Dec. 1985.

12. Sugawara, S., Y. Maita, K. Adachi, K. Mori, and K. Mizuno, "Characteristics of a MM-wave tapered slot antenna with corrugated edges," *IEEE MTT — S Int. Microw. Symp. Dig.*, Vol. 2, 533–536, Jun. 1998.
13. Karthikeya, G. S., M. P. Abegaonkar, and S. K. Koul, "CPW fed wideband corner bent antenna for 5G mobile terminals," *IEEE Access*, Vol. 7, 10967–10975, 2019.
14. <https://mpd.southwestmicrowave.com/wp-content/uploads/2018/06/1092-01A-6.pdf>.
15. Valagiannopoulos, C. A. and N. K. Uzunoglu, "Green's function of a parallel plate waveguide with multiple abrupt changes of interwall distances," *Radio Science*, Vol. 44, No. 05, 1–12, Oct. 2009.
16. Valagiannopoulos, C. A., "Isolating the singular term of the green's function in the vicinity of the corner formulated by two intersecting waveguides," *Microw. Opt. Technol. Lett.*, Vol. 55, 16–23, 2013.
17. Ma, C., Q. Zhang, and E. Keuren, "Right-angle slot waveguide bends with high bending efficiency," *Opt. Express*, Vol. 16, 14330–14334, 2008.
18. Monzon, C., D. W. Forester, and P. Loschialpo, "Exact solution to line source scattering by an ideal left-handed wedge," *Physical Review. E*, Vol. 72, 056606, 2005.
19. Valagiannopoulos, C. A., "On smoothening the singular field developed in the vicinity of metallic edges," *International Journal of Applied Electromagnetics and Mechanics*, Vol. 31, 67–77, 2009.
20. Valagiannopoulos, C. A., "On examining the influence of a thin dielectric strip posed across the diameter of a penetrable radiating cylinder," *Progress In Electromagnetics Research C*, Vol. 3, 203–214, 2008.